

Design of Current Control of Fully Integrated Surface-mounted Permanent Magnet Synchronous Motor Drive Servo Actuators

Xiaofeng Xu, Gerd Hirzinger

Institute of Robotics and Mechatronics of Germany Aerospace Research Center
 Muechener Str. 20
 Oberpfaffenhofen, Germany
 Tel.: +49 / (8153) – 28.3311
 Fax: +49 / (8153) – 28.1134
 E-Mail: Xiaofeng.Xu@dlr.de [Gerd.Hirzinger@dlr.de](mailto>Gerd.Hirzinger@dlr.de)
 URL: <http://www.robotic.de>

Keywords

«Permanent magnet motor», «Integrated adjustable speed drive», «Vector control», «Voltage Source Inverter», «PWM»

Abstract

A stationary frame-based synchronous digital current control for a Surface Mounted Permanent Magnet Synchronous Motor (PMSM) drive of integrated servo actuators is considered. A two phase stator stationary coordinate frame realization synchronous current controller with the anti-windup is presented. A simple implementation of Space Vector PWM algorithms which provide continuous transition from sinusoidal PWM to six-step operation PWM mode is developed to enhance the current dynamic performance.

Introduction

Recently fully integrated adjustable speed drive applications have attracted more attentions for a range of industrial applications. For example, hybrid electric vehicle drives, steer-by wire actuators in the automobile industry, joint actuators in the elastic light weight robots and the machine tool spindle drives. In these applications the PMSM are designed desirably with low inertia, compact configuration and as a result the leakage inductance of motor is rather low in order to get a fast current response. The modern servo drive control demands cycle time of current control lower than $50\mu\text{s}$ for which a compromise between the complexity of the algorithms and the execution time on a micro-processor has to be considered in the implementation of high performance current control.

Current control schemes for a voltage source inverter-fed PM synchronous motor drive can be classified into two categories, namely the stationary frame controller[1][2][3], and synchronous frame controller[4][5]. The State feedback controller which based on dynamically compensation of the EMF voltage can be implemented either in stationary frame [6] or synchronous frame [7]. The synchronous frame controller is generally accepted as an industrial standard. Generally speaking, the stationary frame controller has the advantage of simple implementation. However, there are some unavoidable limitation such as a steady-state current error and phase delay in the steady state which result in the poor performance of the drive system.

In this paper a digital realization of the stationary frame PI current control is presented. The particularity of design the PI controller in stationary frame is addressed. An improved anti-windup PI current is proposed to guarantee both steady and dynamic performance. The whole control system is realized by DSP56807 motion controller for an integrated PM synchronous motor driven by a three phase voltage-fed PWM inverter.

Modeling of PM Synchronous Motor

A PM synchronous motor consists of permanent magnets mounted on the rotor surface and three phase stator windings which are distributed sinusoidally and displaced by 120 deg. The model of the motor can be represented in different frames as follows:

The model of PM synchronous motor in stationary three phase stator frame (S3abc):

$$\begin{bmatrix} L_s & -M & -M \\ -M & L_s & -M \\ -M & -M & L_s \end{bmatrix} * \begin{bmatrix} di_a/dt \\ di_b/dt \\ di_c/dt \end{bmatrix} = \begin{bmatrix} V_a \\ V_b \\ V_c \end{bmatrix} - R \begin{bmatrix} i_a \\ i_b \\ i_c \end{bmatrix} + K_m \omega_m \begin{bmatrix} \sin(n_p \theta_m) \\ \sin(n_p \theta_m - 2\pi/3) \\ \sin(n_p \theta_m + 2\pi/3) \end{bmatrix} \quad (1)$$

Equivalent model in stationary two phase stator frame (S2αβ):

$$\begin{bmatrix} L_s + M & 0 \\ 0 & L_s + M \end{bmatrix} * \begin{bmatrix} di_\alpha/dt \\ di_\beta/dt \end{bmatrix} = \begin{bmatrix} V_\alpha \\ V_\beta \end{bmatrix} - R \begin{bmatrix} i_\alpha \\ i_\beta \end{bmatrix} + \sqrt{\frac{3}{2}} K_m \omega_m \begin{bmatrix} \sin(n_p \theta_m) \\ \cos(n_p \theta_m) \end{bmatrix} \quad (2)$$

Equivalent model in rotor flux oriented rotating frame (R2dq):

$$\begin{bmatrix} L_s + M & 0 \\ 0 & L_s + M \end{bmatrix} * \begin{bmatrix} di_d/dt \\ di_q/dt \end{bmatrix} = \begin{bmatrix} V_d \\ V_q \end{bmatrix} + \begin{bmatrix} -R & n_p \omega_m (L_s + M) \\ -n_p \omega_m (L_s + M) & -R \end{bmatrix} * \begin{bmatrix} i_d \\ i_q \end{bmatrix} + \begin{bmatrix} 1 \\ -\sqrt{3}/2 \end{bmatrix} * \omega_m \quad (3)$$

The current control can be implemented in either of three above different coordinates, namely in stationary frame S3abc, S2αβ or in synchronous frame R2dq.

Stationary Frame Synchronous Current Control

For synchronous frame current regulation (field oriented current control), the synchronous d-q rotating transformation converts a fundamental reference frequency signal into a dc signal. A conventional proportional and integral (PI) controller can be applied to the variables in the rotating reference frame so as to achieve zero steady-state error in response to step command. Then, variables in the synchronous frame must be restored in the stationary frame using inverse d-q rotating transformation. With a stationary frame controller, the entire control loop operates on AC quantities, and is subject to steady-state errors and phase delay with conventional PI controllers. This unavoidable limitation of stationary frame control using traditional PI controllers result in the decrease of the speed range at certain dc supply and deterioration of the efficiency of the drive system. One method with which to increase the speed range over which the desired torque is achieved without increasing the dc link voltage is to implement the PI current control loop in the synchronous reference frame. This synchronous current regulation was originally set forth in [4] for current regulated sine-triangle PWM drives. The overall block diagram for the presented digital current control scheme is shown in Fig.1.

The overall system consists of a stationary frame realization of synchronous PI current controller with a anti-windup compensation unit, A space vector PWM unit and a PM synchronous motor driven by a voltage source inverter. This controller is a synchronous frame current regulator realized in the stationary frame[4] in which all variables are AC quantities. In the conventional PI controller shown in Fig.1 with solid line, it is necessary that a sinusoidally varying error be present to provide a balanced set of ac voltages for operation. The amplitude of the integrator outputs is reduced with the increase of the operating frequency, the phase of the output is also shifted towards 90 deg in mean time. As a result the error tends to become larger and deteriorate the drive performance. The output of two integrators as additional states with phase shifted by 90 deg feed crossingly to the input of the integrators of the other axis as indicated in Fig.1 using by dashed line. These 90 deg phase shifted states compensate the amplitude losses and phase shift in the conventional stationary frame PI controller. In the steady-states the voltages are continuously provided by orthogonal feedback signals, the current error signal can each be equal to zero.

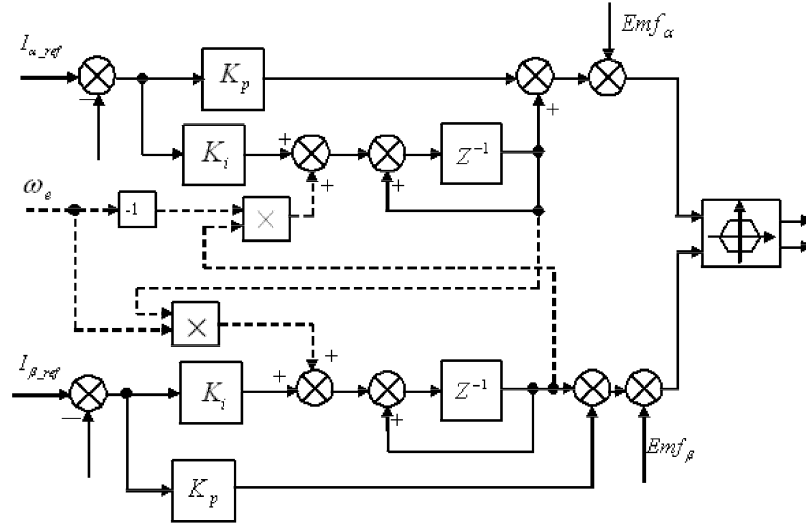


Fig. 1: Overall block diagram for the presented digital current control scheme

Due to the robustness and simplicity in implementation, PI controllers are widely accepted in industrial application. PI controller is discretised using the backward difference method which create two equivalent struture shown in Fig.2

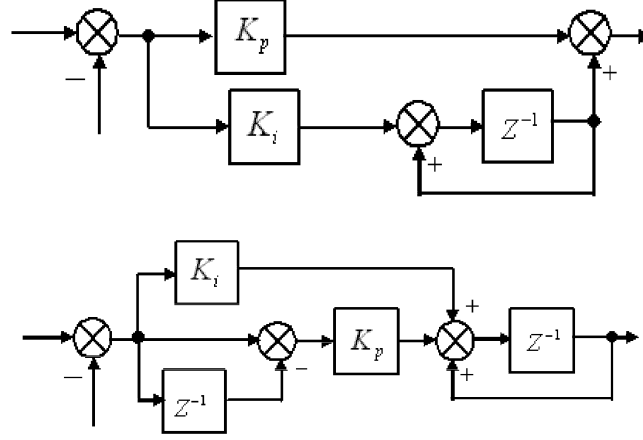


Fig. 2: Digital implementation for the PI controller using the backward difference method

Here the second equivalent is chosen for easier to combine with anti-windup function.

In order to ensure the current control performance at both steady state and transient state, an anti-windup has to be included. In the presented current controller, a PI controller with conditioned ATW is used. The control structure is shown in Fig3.

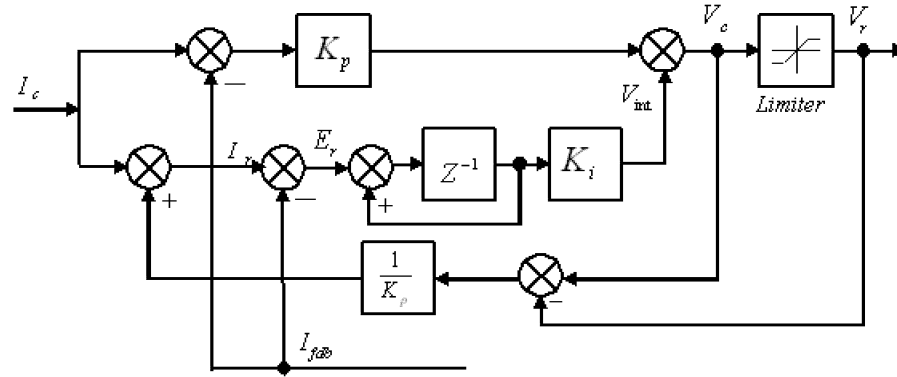


Fig. 3: PI controller with conditioned anti-windup.

In the conditioning ATW controller, when the commanded current I_c applied to the input, the controller produce a commanded voltage V_c which is out of the range of the limiter, error can be created between command V_c and realizable reference V_r , this error is transform to the input of the controller to compare with the command current vector and re-evaluate the new set-point(also called realizable reference) I_r until the consistency between the controller states and control output is restored. Discrete-time PI controller with conditioned ATW can be expressed as:

$$I_r(k-1) = I_c(k-1) + \frac{V_r(k-1) - V_c(k-1)}{K_p} \quad (4)$$

$$V_{int}(k) = V_{int}(k-1) + K_I \{ (I_r(k-1) - I_{fdb}(k-1)) \} \quad (5)$$

$$V_r(k) = V_{int}(k) + K_P \{ I_c(k) - I_{fdb}(k) \} \quad (6)$$

The current response of the presented stationary frame synchronous current controller in response to a step change current command with and without ATW is shown in Fig.4

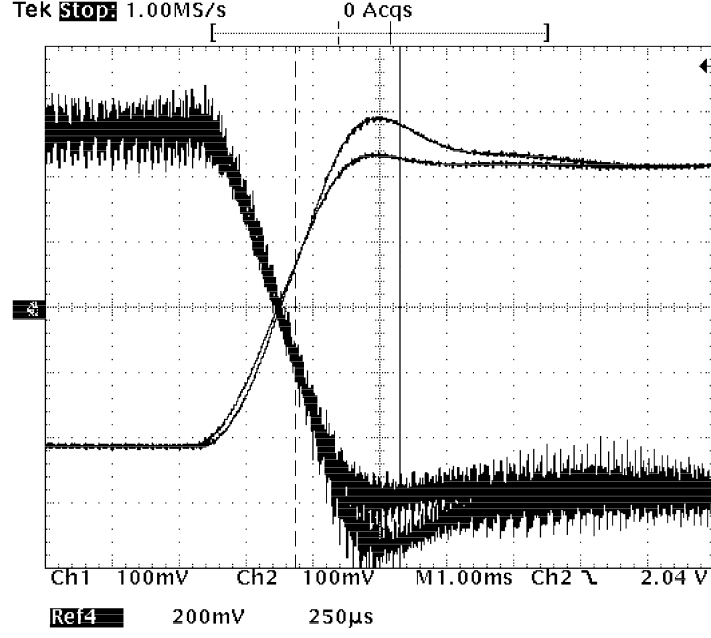


Fig. 4: Rotor locked current response to the step torque command from 1.2 Nm to -1.2Nm PI controller with and without conditioned anti-windup.

The measurement shows the overshoot of the current controller with conditioned anti-windup is apparently be reduced compare with the current controller without conditioned anti-windup.

Design Optimized PWM

It is imperatively important to design a high performance PWM for a high performance current regulation. Compare with the triangular sinusoidal PWM, Space Vector PWM(SVPWM) has the advantage not only in higher utilization of dc link voltage, but also in dynamic over-modulation characteristics. The challenge in implementation SVPWM in fast current control is to simplify its algorithms to meet with the executing time within several micro seconds.

The design of the optimized PWM is shown in Fig.5. As shown in Fig.5, the optimized PWM can be

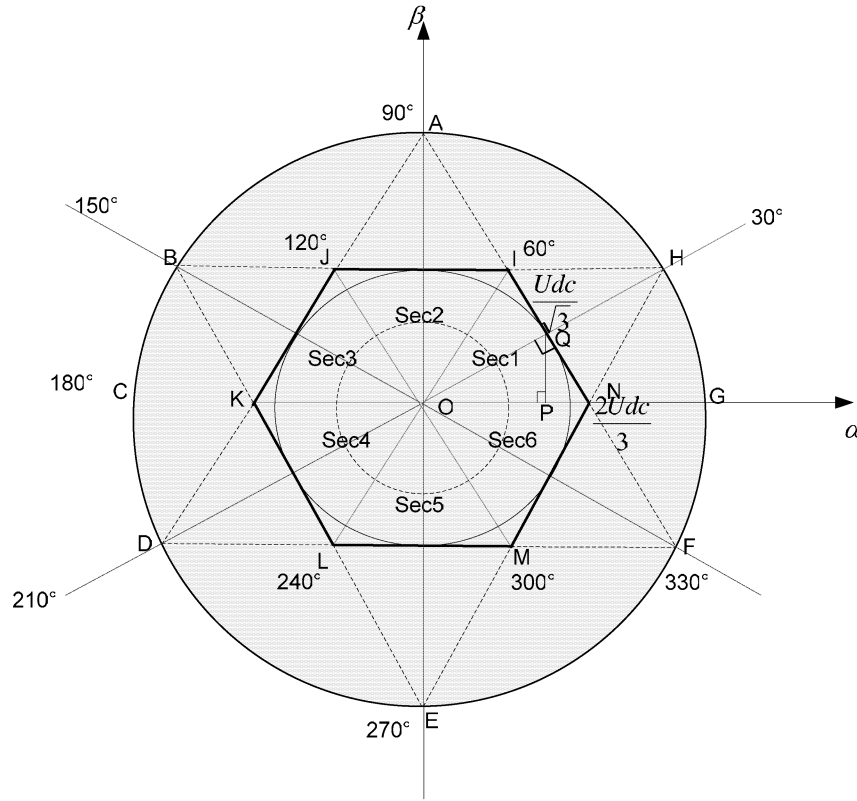


Fig.5 Optimized SVPWM

divided into three region. One region is inside the inner circle depicted in dashed line in where the modulation index is lower than 0.6, the standard space vector PWM is used. In the area between the inner circle and the circle inscribe to the hexagon, discrete PWM is adopted, which means at every instant there are only two phase are switched while the third phase being clamped to either lower or upper dc bus. Unlike standard SVPWM, it gives only one zero state per sampling time. With this discrete PWM, 33% reduction of effective switching frequency can be obtained. In design discrete PWM, the distribution of zero vector is arranged in such a way that from α axis in anti clock wise rotation, $T_7=0$ for the regions $30 \sim 90$ deg, $150 \sim 210$ deg, and $270 \sim 330$ deg while as for $T_0=0$ for $330 \sim 360$ deg, $90 \sim 150$ deg and $210 \sim 270$ deg.

When the calculated reference voltage vectors locate outside the hexagon, which the inverter can not actually provide, the so called over-modulation occurs. In this case the over-modulation algorithms have to be used to restore the realizable voltage vector on the boundary of the hexagon to minimize the error between reference and realizable voltage vector. The over modulation voltage vector limitation method outside the hexagon is designed in such a way that when the demanded voltage vector located in the area of six triangles sit on the edges of hexagon, the equivalent switching time is calculated based on the over modulation method[8], otherwise the six-step mode is adopted.

The calculation of the optimized SVPWM can be simplified using geometric characteristics of Fig.5. The 3 equations which decide zero voltage vector distributions in each sector can be express as:

$$A: u_\beta = \frac{u_\alpha}{\sqrt{3}}; \quad B: u_\alpha = 0; \quad C: u_\beta = -\frac{u_\alpha}{\sqrt{3}}; \quad (7)$$

There are six equations which decide weather or not the reference voltage vector exceeds the inscribed circle of the hexagon and over-modulation occurs:

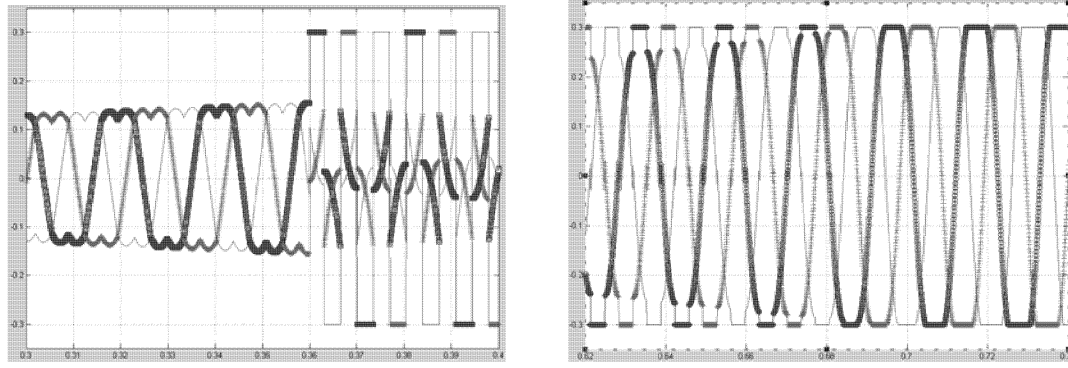
$$\begin{aligned} \text{Sec1: } & \frac{\sqrt{3}}{2}u_\alpha + \frac{1}{2}u_\beta < \frac{U_{dc}}{\sqrt{3}}; & \text{Sec 2: } & u_\beta < \frac{U_{dc}}{\sqrt{3}}; \\ \text{Sec 3: } & \frac{1}{2}u_\beta - \frac{\sqrt{3}}{2}u_\alpha < \frac{U_{dc}}{\sqrt{3}}; & \text{Sec 4: } & -\frac{1}{2}u_\beta - \frac{\sqrt{3}}{2}u_\alpha < \frac{U_{dc}}{\sqrt{3}} \end{aligned} \quad (8)$$

$$\text{Sec 5: } -u_\beta < \frac{U_{dc}}{\sqrt{3}} ; \quad \text{Sec 6: } \frac{\sqrt{3}}{2}u_\alpha - \frac{1}{2}u_\beta < \frac{U_{dc}}{\sqrt{3}}$$

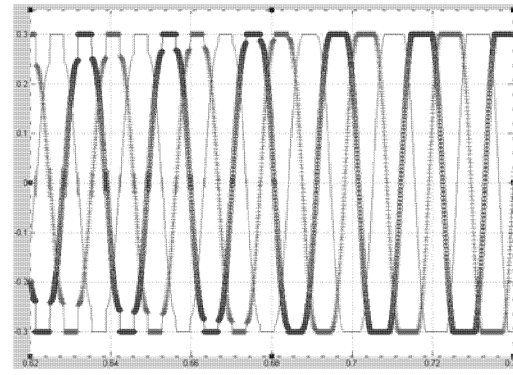
For the transition from over-modulation region to six-step mode operation region, the necessary six decision equitation can be expressed as:

$$\begin{aligned} \text{EH: } u_\alpha + \frac{1}{\sqrt{3}}u_\beta &= \frac{2}{3}U_{dc}; & \text{HB: } u_\beta &= \frac{U_{dc}}{\sqrt{3}}; & \text{FA: } u_\alpha + \frac{1}{\sqrt{3}}u_\beta &= \frac{2}{3}U_{dc} \\ \text{AD: } u_\alpha - \frac{1}{\sqrt{3}}u_\beta &= \frac{2}{3}U_{dc}; & \text{BE: } u_\alpha + \frac{1}{\sqrt{3}}u_\beta &= -\frac{2}{3}U_{dc}; & \text{DF: } u_\alpha + \frac{1}{\sqrt{3}}u_\beta &= \frac{2}{3}U_{dc} \end{aligned} \quad (9)$$

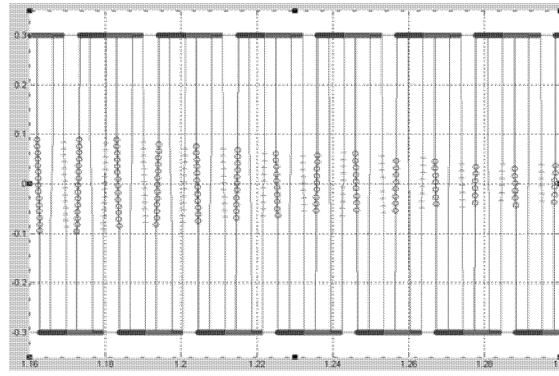
The simulation results of the designed optimum PWM in Fig.6 show that the PWM can continuously



(a). from SVPWM to DPWM



(b). from DPWM to Quasi six-step



(b). from Quasi six-step to full six-step operation

Fig.6 Pole voltage waveform of the inverter at continuous transition from space vector PWM to six-step mode operation

transfer from SVPWM to six-step mode operation. The experiment on continuous transition from the circle inscribed to the hexagon into six-step mode is illustrated in Fig. 7.

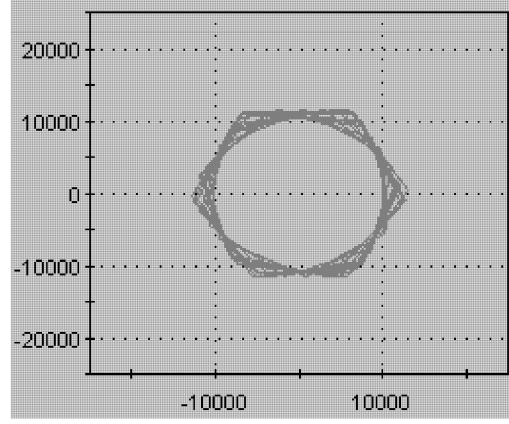


Fig.7 Experiment on continuous transition to six-step mode operation

System Setup and Experiment Results

In addition to the machine, this system consists of a converter, a supervisory current control, and a stationary frame synchronous current control. The supervisory control determines the current command I^* , and the electrical rotor position. The current controller is implemented on a 16bit fix-point DSP56807 which is clocked at 20 kHz and the executing-time of the current control including SVPWM and all I/O operations is within $30 \mu\text{s}$. The supervisory control is established on a float-point DSP TMS320C33 in which control duty cycle is $300 \mu\text{s}$. The two processors communicate with each other through a dual-port RAM. A Sercos chip is responsible for the communication among different joints of the robot. The general setup of the test bench of the motor is illustrated in the Fig. 7. Both supervisory control and motion control are integrated on one Analog-interface board. The supervisory control DSP connects with the dSpace card through a serial interface so that real-time debugging of the controller is feasible. The motor is a 10 pole pair surface mounted permanent synchronous motor with low inertia and compact configuration, on which position sensor and power converter are mechatronically built together.

The photos of the integrated PM synchronous motor system and experiment setup are shown in Fig. 7

The parameters of the PM synchronous motor are listed as follows:

Terminal Resistance: $210 \text{ m}\Omega$; Terminal Inductance: $470 \mu\text{H}$; Rated Voltage: 48
Rated Torque: 1.43 Nm; Rated Power: 450 W; Rated Current: 11 A

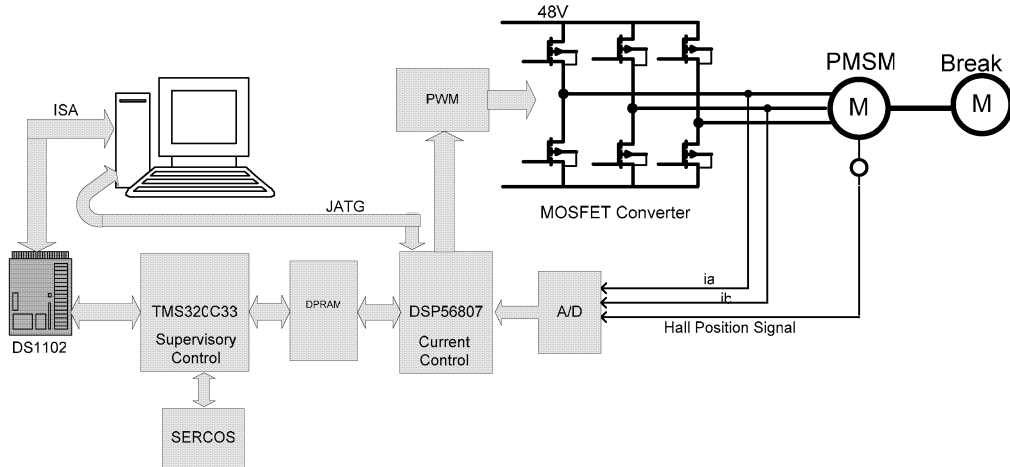
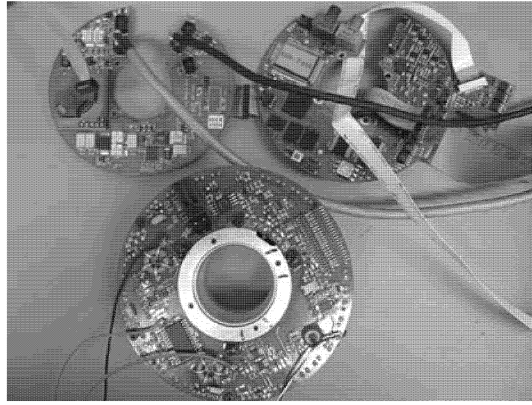
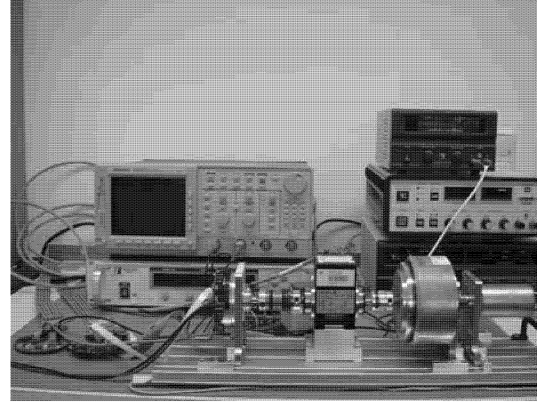


Fig.6 DSP control system block diagram



(a). Motor, Analog interface DSP board and Supply board



(b) Experiment setup

Fig.7 Integrated PM synchronous motor system and experiment setup

In order to verify the performance of the stationary frame synchronous control, a cascaded speed control system is established in which the speed controller is implemented in dSpace, the output of the speed controller $I_{q_{input}}$ serve as the current reference command and is sent to the current controller through serial communication. The experimental phase current oscilloscope waveforms at 2500rpm and 2700 rpm at different load torque are shown in Fig.8

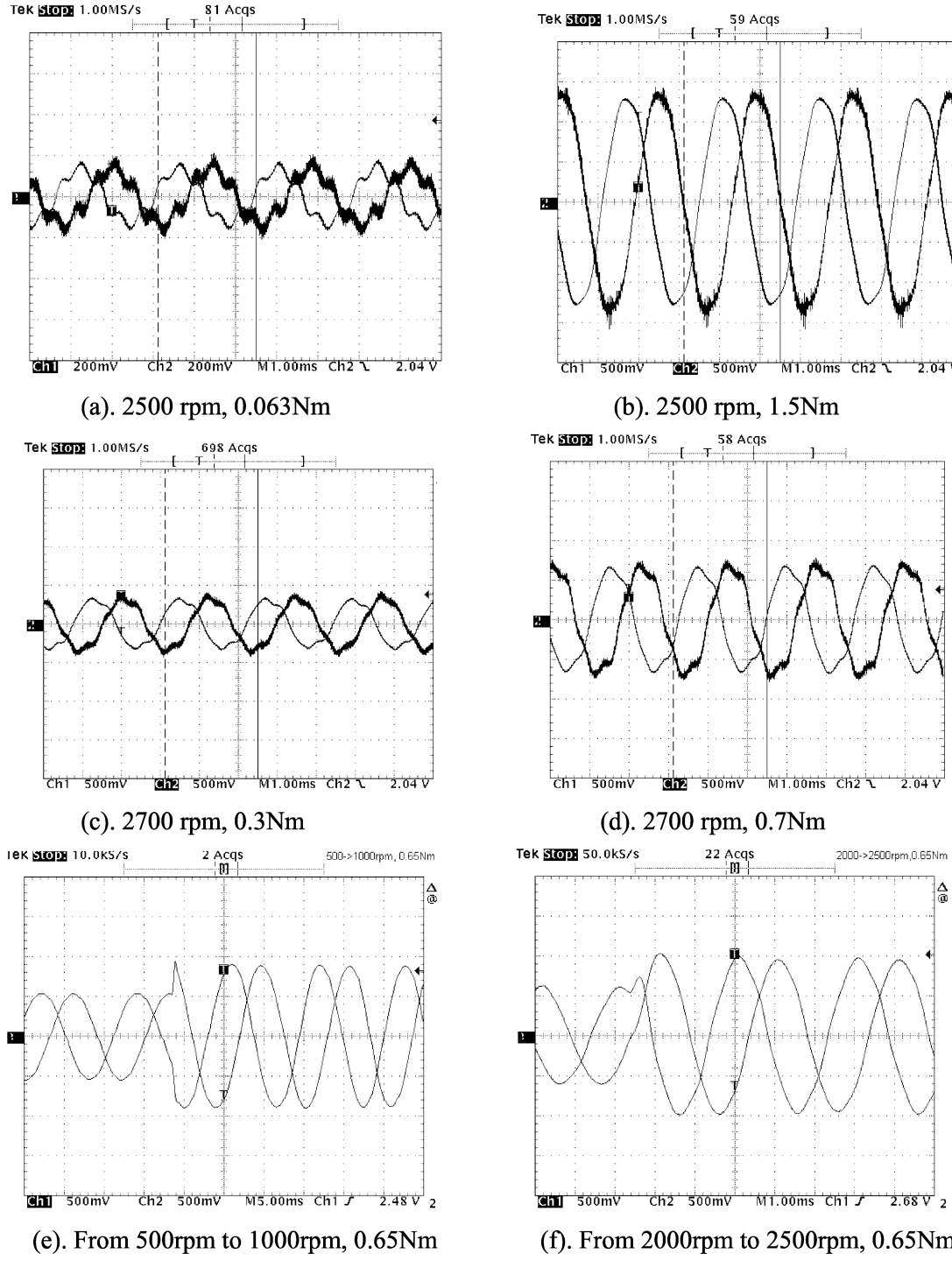


Fig.8 Phase current waveforms at steady-state and transient

Take command torque $I_{q_{input}}$ and output torque as horizontal and vertical axis respectively and the rotation speed as a parameter, the torque performance at difference speed is shown in Fig.9

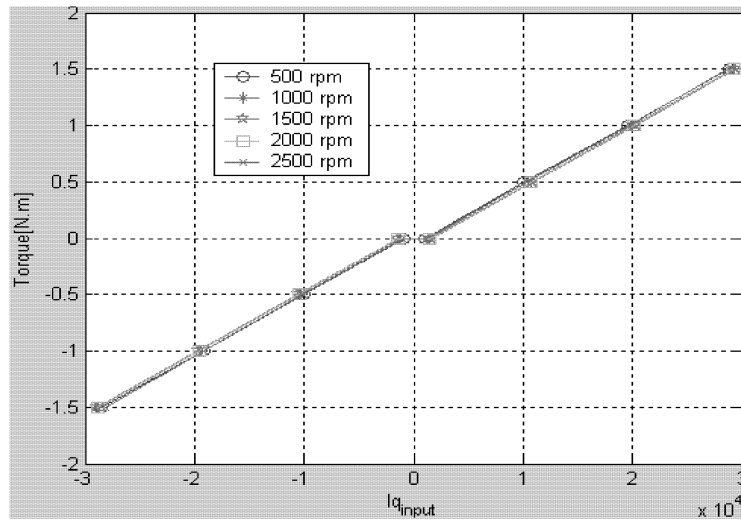


Fig.9 Torque output characteristic of the current controller

From Fig.9 can be seen that at given reference torque, the current controller can provide almost constant torque output at different rotation speed.

Conclusion

In this paper, the realization of a stationary frame synchronous current regulation with anti-windup is introduced. The optimised space vector PWM which is suitable for implementation in servo system is designed. The presented control algorithm is finally realized in the highly integrated PM synchronous motor drive system and is successfully used in the light-weight robots. The experimental results show the feasibility and satisfied performance of the current controller.

References

- [1]. Brod, D.M., and Novotny, D.W. ‘Current Control of VSI-PWM Inverters’, *IEEE Trans. Ind. Appl.*, 1985,21, (4), pp. 562-570.
- [2]. D.N. Zmood, and D.G. Holmes, ‘Stationary Frame Current Regulation of PWM Inverters with Zero Steady State Error’, Conference Proceedings PESC’99, pp. 1185-1190
- [3]. Y.Sato, T. Ishizuka., K. Nezu., and T. Kataoka, ‘A New Control Strategy for Voltage-Type PWM Rectifiers to Realize Zero Steady-State Control Errors in Input Current’, *IEEE Trans. Ind Appl. Vol.34*, No.3, pp. 480-486,1998.
- [4]. T.W. Rowan and R.J. Kerkman, ‘A New Synchronous Current Regulator and an Analysis of PWM Current Regulated PWM Inverters’, *IEEE Trans. Ind Appl. Vol. IA-22*,No. 4, pp678-690, 1986.
- [5]. D.C.Lee, S.K.Sul, and M.H.Park., ‘ High performance current regulator for field-oriented controlled induction motor drive’, *IEEE Trans. Ind Appl. Vol.30*, No.5, pp. 1247-1257.,1994.
- [6]. R.D. Lorenz., and D.B. Lawson, ‘Performance of feed-forward current regulator for field-oriented induction machine controllers’, *IEEE Trans. Ind Appl. Vol. IA-23*, pp597-602, July/Aug. 1987.
- [7]. J.Moerschel, ‘Signal Processor based field oriented Vector Control for an induction motor drive,’ in *Proc EPE Conf.*, Florence Italy, 1991, pp2.145-2.150.
- [8]. J.W.Chi., and S.K.Sul, ‘New Current Control Concept- Minimum Time Current Control in the Three-Phase PWM converter,’ *IEEE Trans. Power Elec. Vol.12*, No.1,pp124- 131.